NeuroImage 171 (2018) 332–340

Contents lists available at ScienceDirect

NeuroImage

journal homepage: www.elsevier.com/locate/neuroimage

# More highly myelinated white matter tracts are associated with faster processing speed in healthy adults

Sidhant Chopra [a], Marnie Shaw [a], Thomas Shaw [a], Perminder S. Sachdev [b], Kaarin J. Anstey [a], Nicolas Cherbuin [a,*]

[a] Centre for Research on Ageing, Health and Wellbeing, Australian National University, Canberra, Australia
[b] Centre for Healthy Brain Ageing, School of Psychiatry, University of New South Wales, New South Wales, Australia

ARTICLE INFO

*Keywords:*
Myelin
Processing speed
White matter
Ageing
T1w/T2w

ABSTRACT

The objective of this study was to investigate whether the estimated myelin content of white matter tracts is predictive of cognitive processing speed and whether such associations are modulated by age. Associations between estimated myelin content and processing speed were assessed in 570 community-living individuals (277 middle-age, 293 older-age). Myelin content was estimated *in-vivo* using the mean T1w/T2w magnetic resonance ratio, in six white matter tracts (anterior corona radiata, superior corona radiata, pontine crossing tract, anterior limb of the internal capsule, genu of the corpus callosum, and splenium of the corpus callosum). Processing speed was estimated by extracting a principal component from 5 separate tests of processing speed. It was found that estimated myelin content of the bilateral anterior limb of the internal capsule and left splenium of the corpus callosum were significant predictors of processing speed, even after controlling for socio-demographic, health and genetic variables and correcting for multiple comparisons. One SD higher in the estimated myelin content of the anterior limb of the internal capsule was associated with 2.53% faster processing speed and within the left splenium of the corpus callosum with 2.20% faster processing speed. In addition, significant differences in estimated myelin content between middle-age and older participants were found in all six white matter tracts. The present results indicate that myelin content, estimated *in vivo* using a neuroimaging approach in healthy older adults, is sufficiently precise to predict variability in processing speed in behavioural measures.

## 1. Introduction

The highly-myelinated nature of the human brain and the vulnerability of myelin to degeneration, may contribute to our species' susceptibility to age-related neurocognitive disorders. The cognitive domain most associated with myelin is processing speed (PS) (Lu et al., 2011, 2013) – a sensitive indicator of overall cognitive decline (Finkel et al., 2007; Cherbuin et al., 2010). It has been demonstrated that PS is the basic cognitive mechanism that mediates age-related decline in memory (Bunce and Macready, 2005; Lee et al., 2012). PS can be conceptualised as the rate at which cognitive operations are executed, such as planning and initiation of intended motion and is often tested in conjunction with psychomotor speed, which accounts for the speed of the motion itself (Cepeda et al., 2013). Recent longitudinal studies have demonstrated an inverse U-shaped lifespan trajectory of myelin content with a peak at around 30–40 years (Bartzokis et al., 2012). A similar trajectory has been observed in cognitive PS scores across the lifespan (Cerella and Hale, 1994; Bartzokis et al., 2010). Further, a decline in PS is the primary cognitive deficit underlying the rapid cognitive decline seen in demyelinating diseases such multiple sclerosis (Demaree et al., 1999). In addition, myelin loss and PS decline have also been shown to share multiple risk-factors including *APO*E4* genotype (Bartzokis et al., 2007), and lifestyle factors (Anstey et al., 2009; Ramagopalan et al., 2010).

A few studies have made important contributions in this area by using indirect imaging measures such as transverse relaxation rate or diffusion measures such as fractional anisotropy. Such studies on healthy older populations have found that the integrity of white matter regions, especially in frontal areas, are correlated with PS, and that these regions show modest mediation effects on age-related PS decline (Lu et al., 2011, 2013; Salami et al., 2012). These studies have used a maximum of two PS tests and as such are potentially confounded by unwanted variance relating to other cognitive domains (Salthouse et al., 1996). Other

* Corresponding author. Centre for Research on Ageing, Health and Wellbeing, 54 Mills Road, Australian National University, Canberra, ACT 2601, Australia.
*E-mail addresses:* sid.chopra@monash.edu (S. Chopra), marnie.shaw@anu.edu.au (M. Shaw), t.shaw@uq.edu.au (T. Shaw), p.sachdev@unsw.edu.au (P.S. Sachdev), kaarin.anstey@anu.edu.au (K.J. Anstey), nicolas.cherbuin@anu.edu.au (N. Cherbuin).

https://doi.org/10.1016/j.neuroimage.2017.12.069
Received 8 August 2017; Accepted 21 December 2017
Available online 22 December 2017

research using more robust measures of PS have shown more global effects by demonstrating that general factor of white matter fractional anisotropy is able to predict PS in healthy older adults (Penke et al., 2010; Kerchner et al., 2012). However, the measures of white matter integrity used by these studies are unspecific as they index the movement of water molecules which are affected, apart from myelin, by neuronal and glial density and size (Winston, 2012), as well as pathological states such as amyloid beta deposition (Racine et al., 2014).

In addition, few such studies have accounted for hemispheric asymmetries in myelin content of white matter tracts in healthy adults (Toga and Thompson, 2003; Takao et al., 2011). These asymmetries have been shown to be associated with specialisations in language, memory and motor functions, and as such may indeed be implicated in PS (de Schotten et al., 2011; Ocklenburg et al., 2016). For instance, the corpus callosum is the primary tract that facilitates information transfer between hemispheres and asymmetrical myelin content may differentially disrupt speed and efficiency of communication between and within networks. In particular, tracts within the left hemisphere have been repeatedly shown to be more susceptible to age- and pathology-related neurodegeneration (Thompson et al., 2007; Minkova et al., 2017). Accounting for such asymmetries in myelin content will assist in clarifying how tracts within each hemisphere differentially contribute to age-related changes in PS.

Few studies have directly examined the relationship between myelin content and PS in non-clinical populations, and we are not aware of any study using a measure specifically developed for this purpose. This is likely due to the difficulty in measuring myelin levels *in vivo*. Histological myelin measurement is the gold standard, but it can only be performed post-mortem and is therefore not suitable to investigate this question in humans.

Recently, a new measure, the ratio between an individual's structural T1-weighted (T1-w) and T2-weighted (T2-w) image (T1w/T2w), has been proposed as a practical and sensitive measure for *in vivo* myelin content estimation (Glasser and Van Essen, 2011; Ganzetti et al., 2014). Multiple studies have demonstrated that T1w/T2w cortical intensity maps parallel myeloarchitectural maps based on histological samples (Glasser and Van Essen, 2011; Ganzetti et al., 2014, 2015; Glasser et al., 2014; Nieuwenhuys and Broere, 2017). Recently, an immunocytochemistry study of post-mortem brains showed that T1w/T2w values correlate with myelin levels (Nakamura et al., 2017). The T1w/T2w ratio has also been used to estimate *in vivo* myelin degeneration in patients with schizophrenia (Ganzetti et al., 2015; Iwatani et al., 2015), multiple sclerosis (Beer et al., 2016), and bipolar disorder (Ishida et al., 2017). Further, the method has been used to demonstrate that higher estimated myelin within the cerebral cortex is associated with reduced intra-subject variability on speeded tasks (Grydeland et al., 2013).

Although we are not aware of any research investigating the association between sub-cortical myelin content (MYE) as estimated by T1w/T2w, and cognitive performance, we predicted based on the available literature that lower MYE within white matter tracts would be associated with lower PS in cognitively healthy individuals. Moreover, since age-related decrease in brain myelin has been clearly demonstrated (Bartzokis, 2004), we predicted that older individuals would present with lower MYE levels than younger individuals and that this difference would be associated with a slower PS. Thus, the aim of this study was to investigate whether MYE of major white matter tracts was predictive of PS in a large sample of cognitively healthy middle-age and older adults.

## 2. Materials and method

### 2.1. Participants

Participants were selected from the MRI sub-study within the PATH Through Life Project (PATH) which has been described in detail elsewhere (Anstey et al., 2012). Briefly, PATH is an ongoing population-based longitudinal study that aims to track the course of cognitive ability, mental health disorders, substance use and dementia across the lifespan. Participants are randomly selected from the electoral roll of the Australian Capital Territory and surrounding regions. Data collection started in 1999 and participants are reassessed every four years.

The PATH study consists of three cohorts: 20–24 years (young adult), 40–44 years (middle-age), and 60–64 (older-age) years at baseline. The focus of this study is on the middle-age (MA) and older-age (OA) cohorts at the third assessment, due to the availability of higher quality T1-w and T2-w MRI scans for both the MA and OA participants at this time-point. Of the 2530 MA and 2550 OA participants recruited into the study, 304 MA and 303 OA participants had complete imaging data at the third assessment. However, an inhouse quality control script and visual inspection revealed an additional 14 scans that were excluded due to poor quality. From this sample, a further 23 participants were excluded due to: epilepsy ($n = 2$), having a history of stroke ($n = 14$), Parkinson's disease ($n = 3$), dementia ($n = 2$) and cognitive impairment ($n = 2$) as defined by a Mini-Mental Status Exam score of less than 25. The final sample available for analysis included 570 participants (277 MA and 293 OA). The selected sample did not differ significantly from the overall MA and OA PATH cohort on sex and education; however, it was significantly younger ($t = 1.967$, $p = .049$).

### 2.2. Socio-demographic, health and genetic measures

Years of education, alcohol consumption, smoking, physical activity were assessed using self-report. Alcohol consumption was assessed as the number of standard alcoholic drinks consumed per week (Alcohol Use Disorders Identification Test; Babor et al., 2001). Physical activity was assessed as the number of hours per week of mild, moderate and vigorous exercise. To provide an intensity-sensitive continuous score of physical exercise, the three levels of activity were combined using a weighted procedure such that hours of mild physical activity were multiplied by 1, hours of moderate physical activity by 2 and hours of vigorous physical activity by 3 (Lamont et al., 2014). Depressive symptomology was assessed using the Goldberg Depression Score (Goldberg et al., 1988). Seated systolic and diastolic blood pressures (BP) were averaged over two measurements after a 5-min rest and participants were classified as hypertensive if they were on medical therapy for hypertension or if they had an average systolic BP $\geq$ 140 mm Hg or diastolic BP $\geq$ 90 mm Hg. Genomic DNA was extracted using cheek swabs and was used to identify the presence of *APO*E4* genotype (Christensen et al., 2008).

### 2.3. Measures of cognitive PS

PS was assessed using five different tasks. The Symbol Digit Modalities Test (SDMT; Strauss et al., 2006), was scored as the number of correct matches identified according to the stimulus symbol digit code, within a 90-s period. Simple (SRT) and choice reaction time (CRT) were assessed by giving participants a small box to hold with both hands, with left and right buttons at the top to be depressed by the index fingers. The front of the box had three lights: a red stimulus light under each of the left and right buttons, and a green get-ready light in the middle. For SRT task, participants placed their right hand, on the right button and were asked to press it as quick as possible when they saw the red stimulus light up. For the CRT task, participants were asked to place their right finger on the right button and their left finger on the left button and to press the corresponding button when the left or right red light lit up. There were 4 blocks of 20 trials measuring SRT, followed by two blocks of 20 trials measuring CRT. The mean reaction time was the average across all trials. Trail Making Task Part A (TMT-A; Reitan, 1958) was scored as the amount of time taken to complete the task and the Purdue Pegboard task using both hands (PP; Tiffin and Asher, 1948) was scored as the number of pairs of pins placed into the pegboard device within 30-s.

### 2.4. MRI data acquisition

All participants were imaged in a 1.5-T Siemens Avanto scanner (Siemens Medical Solutions, Erlangen, Germany). It has been shown that after calibration procedures are implemented (described in the following section), the T1w/T2w values obtained from 1.5-T scans are similar to those obtained at 3-T (Ganzetti et al., 2014). T1-w images were acquired in sagittal orientation with (repetition time/echo time/flip angle/slice thickness = 1160ms/4.17ms/15°/1 mm) matrix size $256 \times 256$ and voxel size of $1 \times 1$ mm. T2-w images were acquired in coronal orientation with (repetition time/echo time/flip angle/slice thickness = 9680ms/115ms/150°/4 mm) matrix size $256 \times 256$ and voxel size $0.898 \times 0.898$ mm.

### 2.5. MRI data analysis

T1-w and T2-w image were pre-processed and combined, following the method and workflow outlined in Ganzetti et al. (2014, 2015). This process included bias correction and intensity calibration on both the T1-w and T2-w image before they were combined. This entire process was undertaken using Freesurfer, FSL and the MINC imaging toolbox (http://www.bic.mni.mcgill.ca/ServicesSoftware).

First the T1-w images were transformed using the MNI152 atlas into Talairach space. A rigid-body transform was then used to match the T2-w image to the already transformed T1-w image. To address intensity bias due to distortions in the B1 field between T1-w and T2-w images, each image was first individually bias-corrected using the mri_nu_correct.mni tool from the MINC imaging toolbox (http://www.bic.mni.mcgill.ca/ServicesSoftware) with the default setting. As the T1w/T2w technique is a qualitative technique, it is susceptible to intensity scaling discrepancies across both individuals and scanners. As such, a calibration procedure recommended by Ganzetti et al. (2014) which corrects for these discrepancies was implemented. The procedure involves a linear transformation of the bias-corrected images. Specifically, two non-brain areas of homogenous intensity were selected: one area that contains relatively high values in the T1-w scan and relatively low values in the T2-w scan, and another area with the reverse characteristics. Consistent with Ganzetti et al. (2014), the temporal muscle and the eyeball humour were selected. To calculate the scaling factors, the mode value in each of the selected areas was extracted and compared with corresponding values from the high-resolution International Consortium for Brain Mapping (ICBM) reference image. The T1-w and T2-w images were then separately multiplied by the resulting scaling factor to create the calibrated images. After calibration, the T1-w image was divided by the T2-w image to create the final T1w/T2w ratio image.

### 2.6. Regions of interest

Consistent with previous research on myelin content (Whittall et al., 1997; Leppert et al., 2009; Welker and Patton, 2012; Ganzetti et al., 2014) and involvement in cognition (Madden et al., 2004; Turken et al., 2008; Davis et al., 2009; Salami et al., 2012), a total of 6 white matter tracts with putatively high myelin content were selected: anterior corona radiata (ACR), superior corona radiata (SCR), pontine crossing tract (PCT), anterior limb of the internal capsule (ALIC), genu of the corpus callosum (GCC), splenium of the corpus callosum (SCC). All ROIs were defined using the stereotaxic single-subject manually parcellated (Type I; threshold of fractional anisotropy > 0.25) John Hopkins University white-matter tractography atlas (JHU-DTI-SS; Oishi et al., 2009),which is a part of the FSL atlas tools (see Fig. 1 for visual representation of ROIs). In order to precisely align with the T1w/T2w images, the atlas was affine-aligned into MNI152 space. The image containing labels for individual tracts was accordingly transformed to subject space. The mean MYE (per tract) was computed as the mean intensity of all voxels with the tract.

Light blue = anterior corona radiata, dark blue = superior corona radiata, red = anterior limb of the internal capsule, magenta = genu of the corpus callosum, green = splenium of the corpus callosum, yellow = pontine crossing tract. ROIs were defined using the manually parcellated (Type I) John Hopkins University white-matter tractography atlas (JHU-DTI-SS; Oishi et al., 2009).

### 2.7. Statistical analysis and experimental design

Statistical analyses were computed using IBM SPSS Statistics 24. Age was split into two variables to separately assess the within and between cohort variability in age: age group (AgeG) and age centred (AgeC). AgeG indicated whether the participant belonged to the MA or OA group. AgeC was calculated by subtracting the rounded age of the youngest participant from the exact age of participants in each group. After being converted to z-scores, the five different tests of PS were subject to a principal component analysis (PCA) in order to extract a single common factor of PS. Principal components with an eigenvalue greater than 1 were retained for further consideration. The selected principal component of PS was confirmed by the high and consistent loadings of individual measures of PS contributing to it. For ease of interpretation, the scores were inverted (multiplied by -1), so that higher scores on the factor correspond to faster PS.

Independent sample t-tests and chi-squared tests were used to assess AgeG differences between the MA and OA groups on socio-demographic, health, genetic variables. Multiple paired sample t-tests were used to assess inter-subject differences within mean T1w/T2w values for the

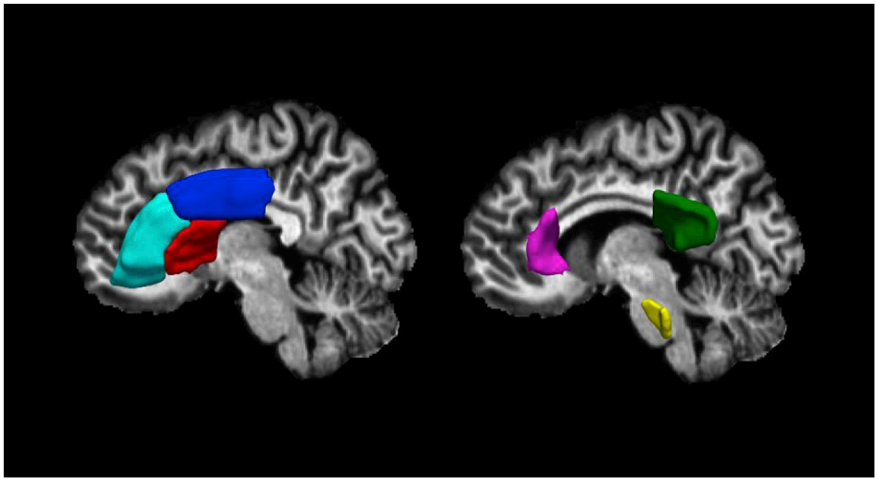

**Fig. 1.** Visual representation of ROIs (left hemisphere).

selected ROIs. Multiple ANCOVAs were used to identify AgeG and Sex differences and interactions in MYE, controlling for AgeC, within the six white matter tracts. The same approach was used to identify AgeG and Sex differences in the principal component of PS.

To assess whether MYE could predict PS, hierarchical linear regression analyses were performed to examine the association between MYE and PS. The preliminary model included AgeG, AgeC, Sex and Education as independent variables and PS as the dependent variable (block 1). MYE of the ROI and a lateralization index [calculated with the formula [(L-R)/(L + R)*100] were entered as an independent variable (block 2). To determine whether mean ROI intensity could account for any additional variance in PS over health and genetic variables (alcohol consumption, smoking, physical activity, hypertension, presence of APO*E4 genotype and depressive symptomology), block 3 included all variables examined. The lateralization index was only retained in the models if it was a significant predictor. All two-way and three-way interactions terms involving AgeG, AgeC, Sex and MYE were examined (block 4). Significance was set at $p < .05$ and correction for multiple comparisons was applied using the sequential Holm-Bonferroni method (Holm, 1979). Analyses using individual tests of PS were corrected for 5 comparison and the main regression analyses using individual tracts were corrected for 6 comparisons. Unadjusted p-values are reported for all analyses.

## 3. Results

### 3.1. Sample characteristics

Group comparison between the OA and MA groups revealed that the OA group had fewer females, was significantly less educated, had a higher physical activity score, higher rates of hypertension and scored higher on depressive symptomology (Table 1).

### 3.2. Comparison of mean T1w/T2w values within ROIs

Significant differences in the mean T1w/T2w values were found between all tracts ($t = 4.967$ to 45.308, $p < .001$), apart from between the ALIC and GCC ($t = 1.330$, $p = .184$). Sample means and SDs are listen in Table 1, and effect sizes ranged from Cohens $d = 0.086$ (ACR and PCT) to Cohens $d = 0.313$ (SCC and PCT).

### 3.3. Age group and sex differences in MYE

The Tract by AgeG by Sex ANCOVA revealed the following effects. A main effect for AgeG was detected, indicating that the OA group had significantly lower MYE in all six of the white matter tracts examined (Table 1), with large effect sizes: ACR ($F = 1130.177$, $p < .001$, $\eta_p^2 = 0.671$), SCR ($F = 1644.536$, $p < .001$, $\eta_p^2 = 0.746$), PCT ($F = 991.323$, $p < .001$, $\eta_p^2 = 0.639$), ALIC ($F = 1026.559$, $p < .001$, $\eta_p^2 = 0.647$), GCC ($F = 1041.574$, $p < .001$, $\eta_p^2 = 0.651$) and SCC ($F = 1052.399$, $p < .001$, $\eta_p^2 = 0.655$). On average, the white matter tracts of the OA group had 21.95% less MYE when compared to the MA group, with the biggest difference seen in the SCR (24.08%) and the ALIC (24.06%), followed by ACR (22.11%), GCC (22.04%) SCC (20.23%) and PCT (19.17%).

A significant main effect of sex was found within the SCC ($F = 5.822$, $p = .016$, $\eta_p^2 = 0.010$), with females having 1.60% less MYE than males. An AgeG by Sex interaction was detected in the ALIC ($F = 6.305$, $p = .012$, $\eta_p^2 = 0.011$), SCR ($F = 4.447$, $p = .035$, $\eta_p^2 = 0.008$), ACR ($F = 4.000$, $p = .046$, $\eta_p^2 = 0.007$) and the PCT ($F = 4.849$, $p = .028$, $\eta_p^2 = 0.009$). In all cases, females had higher levels of MYE in the MA group, but lower in the OA group. Fig. 2 shows age and sex differences in MYE.

### 3.4. Principal component of PS

A principal component analysis (PCA) was run on the five PS tasks in order to extract a single component of PS. The PCA revealed one factor that had an eigenvalue greater than one ($\lambda = 2.86$) and which explained 57.50% of the total variance. Loadings for each test were as follows (with communalities in parentheses): CRT = 0.842 (70.9%), SDMT = −0.803 (64.4%), SRT = 0.761 (57.9%), TMT-A = 0.721 (52.0%) and PP = −0.650 (42.3%). Consequently, as expected this component was

**Table 1**
Sample characteristics and age-group differences.

| Variable | Overall sample | Age group comparison | | | |
|---|---|---|---|---|---|
| | | Middle-Age | Older-age | T or $\chi^2$ | *p* |
| Age, years (SD) | 61.47 (9.92) | 51.21 (1.36) | 70.89 (1.39) | −120.43 | **<.001**** |
| Range | 48.63–73.78 | 48.63–53.86 | 68.55–73.78 | | |
| Females, N (%) | 327 (49.55) | 170 (53.8) | 157 (45.6) | **4.39** | **.036*** |
| Education, years (SD) | 14.43 (2.53) | 14.91 (2.22) | 14.02 (2.70) | **4.54** | **<.001**** |
| Physical activity score (SD) | 47.44 (42.72) | 39.71 (34.69) | 53.05 (46.72) | **−4.07** | **<.001**** |
| Smoking History or Current, N (%) | 290 (43.9) | 146 (46.2) | 114 (41.9) | 1.26 | .262 |
| Alcohol Consumption (SD) | 6.34 (7.75) | 6.21 (7.82) | 6.64 (7.84) | −0.69 | .491 |
| Hypertension, N (%) | 385 (58.30) | 114 (36.1) | 271 (78.8) | **123.57** | **<.001**** |
| ApoE ε4, N (%) | 175 (26.5) | 88 (27.8) | 87 (25.3) | .533 | .457 |
| Depression score (SD) | 1.87 (2.13) | 2.19 (2.32) | 1.57 (1.90) | **3.69** | **<.001**** |
| Tests of PS | | | | | |
| SDMT, mean (SD) | 54.13 (10.75) | 60.55 (8.26) | 48.39 (9.21) | **17.52** | **<.001**** |
| SRT, mean (SD) | 261.48 (67.61) | 236.21 (49.98) | 283.90 (73.34) | **−9.52** | **<.001**** |
| CRT, mean (SD) | 319.89 (60.55) | 292.73 (47.99) | 343.59 (59.97) | **−11.77** | **<.001**** |
| TMT-A, mean (SD) | 31.39 (10.90) | 25.63 (7.02) | 36.65 (10.96) | **−14.98** | **<.001**** |
| PP, mean (SD) | 10.62 (2.21) | 11.80 (1.84) | 9.48 (1.91) | **15.65** | **<.001**** |
| LPS | 0.00 (1) | 0.66 (0.67) | −0.59 (0.87) | **19.93** | **<.001**** |
| T1w/T2w mean intensity | | | | | |
| ACR, mean (SD) | 1.76 (0.27) | 1.99 (0.11) | 1.55 (0.19) | **33.67** | **<.001**** |
| SCR, mean (SD) | 1.68 (0.27) | 1.91 (0.10) | 1.45 (0.16) | **40.50** | **<.001**** |
| PCT, mean (SD) | 1.74 (0.23) | 1.93 (0.09) | 1.56 (0.17) | **31.65** | **<.001**** |
| ALIC, mean (SD) | 1.64 (0.28) | 1.87 (0.12) | 1.42 (0.20) | **32.00** | **<.001**** |
| GCC, mean (SD) | 1.65 (0.25) | 1.86 (0.11) | 1.45 (0.18) | **32.30** | **<.001**** |
| SCC, mean (SD) | 1.55 (0.21) | 1.73 (0.10) | 1.38 (0.14) | **32.43** | **<.001**** |

Abbreviations: PS = processing speed; LPS = latent factor of processing speed; SDMT = Symbol Digits Modalities Test; SRT = simple reaction time; CRT = choice reaction time; TMT-A = Trial Making Task A, PP = Purdue Pegboard; ACR = anterior corona radiata; SCR = superior corona radiata; PCT = pontine crossing tract; ALIC = anterior limb of the internal capsule; GCC = genu of the corpus callosum; SCC = splenium of the corpus callosum. Significant p-values and corresponding T or χ2 values are given in bold.
* Significant at $p < .05$.
**Significant at $p < .001$.

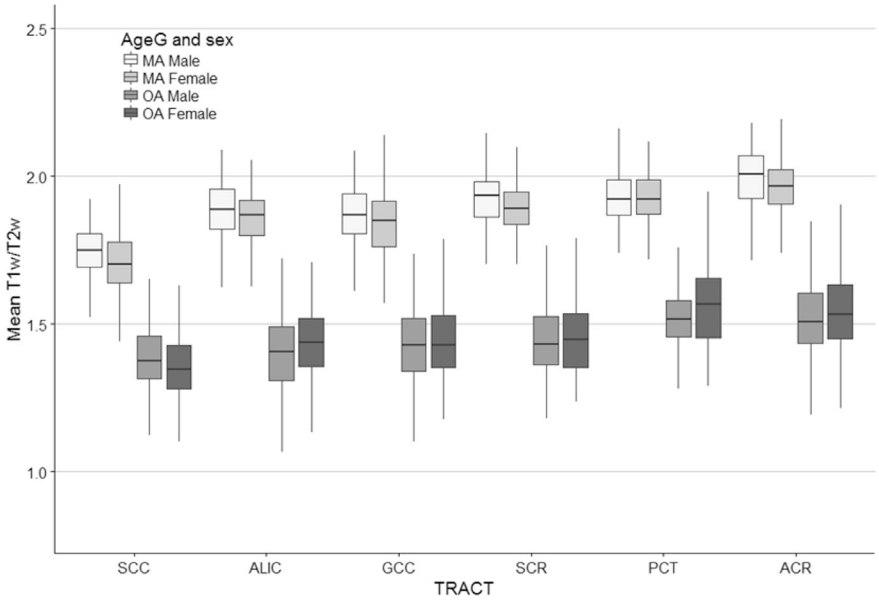


**Fig. 2.** Age group (AgeG) and sex differences in estimated tract myelin content. This Tukey boxplot (showing median values, upper and lower quartiles and 1.5 interquartile ranges) demonstrates that on average middle-ages participants (MA) had higher estimated myelin levels (MYE) than older-aged participants (OA) and that while females had higher MYE in MA within ALIC, SCR and ACR, they presented with lower levels in OA within these three tracts. Additionally, the finding that the GCC has higher MYE than the SCC is consistent with previous histological findings (Aboitiz et al., 1992). ACR = anterior corona radiata; SCR = superior corona radiata; PCT = pontine crossing tract; ALIC = anterior limb of the internal capsule; GCC = genu of the corpus callosum; SCC = splenium of the corpus callosum.

interpreted as reflecting a latent factor of PS (LPS) and for ease of interpretation was inverted, with higher scores representing faster speeds.

### 3.5. Age group and sex differences in PS

The AgeG by Sex ANCOVAs testing performance on LPS revealed a significant main effect of AgeG, with the OA group performing slower on average, with a large effect size ($F = 355.262$, $p < .001$, $\eta_p^2 = 0.394$). No significant main effect for Sex or interaction effects were detected.

To determine whether individual measures contributed differently to these effects, follow-up analyses revealed a significant main effect of AgeG on all individual tests of PS: SDMT ($F = 262.738$, $p < .001$, $\eta_p^2 = 0.323$), Trails A ($F = 204.662$, $p < .001$, $\eta_p^2 = 0.268$), SRT ($F = 84.670$, $p < .001$, $\eta_p^2 = 0.134$), CRT ($F = 131.251$, $p < .001$, $\eta_p^2 = 0.189$), PP ($F = 207.150$, $p < .001$, $\eta_p^2 = 0.269$). Significant main effect of Sex revealed that females performed faster for SDMT ($F = 4.849$, $p = .043$, $\eta_p^2 = 0.007$) and PP ($F = 33.525$, $p < .001$, $\eta_p^2 = 0.053$), and slower for CRT ($F = 6.733$, $p = .004$, $\eta_p^2 = 0.015$) and SRT ($F = 8.500$, $p = .002$, $\eta_p^2 = 0.017$). The differences in Pegboard, CRT and SRT survived Holm-Bonferroni correction for multiple comparisons. No significant interaction effects were detected.

### 3.6. MYE as a predictor of PS

Hierarchical regression modelling revealed that higher MYE significantly predicted faster PS but only in the ALIC (Table 2). One SD higher in the MYE of the ALIC was associated with 2.53% higher PS. This was a robust finding as the association remained significant after controlling for all covariates and after Holm-Bonferroni correction for multiple comparisons. Associations in all other white matter tracts followed a similar trend but did not reach significance. No significant interactions were detected. Scatterplots of PS as a function of MYE for each tract are presented in Fig. 3.

### 3.7. Age as a predictor of PS

AgeG remained a significant predictor of PS in all six of the final models, with membership of the OA group resulting in a 16.56%–19.42% slower PS depending on which tract was entered. The effect of AgeG survived Holm-Bonferroni correction for multiple comparison in all models. AgeC also remained a significant predictor in all final models, indicating that one-year higher in age within age groups was associated with a 0.95%–1.03% slower PS, depending on which tract was entered into the models. However, this effect did not survive Holm-Bonferroni correction for multiple comparisons. No significant interactions between AgeG, AgeC were detected.

**Table 2**
Hierarchical linear regression testing associations between myelin content and PS.

| ROI | Model 1[a] | Model 2[a,b] | | | Model 3[a,b,c] | | |
|---|---|---|---|---|---|---|---|
| | $R^2$ | $\Delta R^2$ | β | *p* | $\Delta R^2$ | β | *p* |
| ACR | .421 | .002 | .340 | .158 | .014 | .362 | .132 |
| SCR | .410 | .002 | .353 | .148 | .014 | .363 | .137 |
| PCT | .411 | .004 | .394 | .063 | .014 | .405 | .052 |
| ALIC | .410 | .007 | **.519** | **.009**** | .014 | **.526** | **.008**** |
| GCC | .410 | .003 | .387 | .081 | .014 | .433 | .050 |
| SCC | .418 | .011 | .275 | .319 | .015 | .304 | .270 |

** Significant at $p < .01$. Significant p-values and corresponding β values are given in bold.
[a] Model includes AgeG, AgeC, Sex and Education.
[b] Model includes MYE (mean T1w/T2w) of ROI and the laterality index. As the laterality index was dropped from the model unless it was a significant predictor, it was removed from all models except for SCC models.
[c] Model includes alcohol consumption, smoking, physical activity, hypertension, presence of APO*E4 genotype, depressive symptomology.

### 3.8. Sex as a predictor of PS

Sex was not a significant predictor in any of the six models. However, a trend suggested females performed 1.23%–1.59% faster than males, depending on which tract was entered into the models. No significant interactions involving sex were detected.

### 3.9. Post-hoc analyses

#### 3.9.1. Hemispheric differences in MYE

In order to better understand the role of myelin content in PS, we conducted further analyses to investigate whether there were hemispheric differences in MYE and whether hemispheric asymmetries contribute to the effects detected above.

Analyses revealed a significant main effect for hemisphere within all tracts, with the left hemisphere having lower MYE than the right within

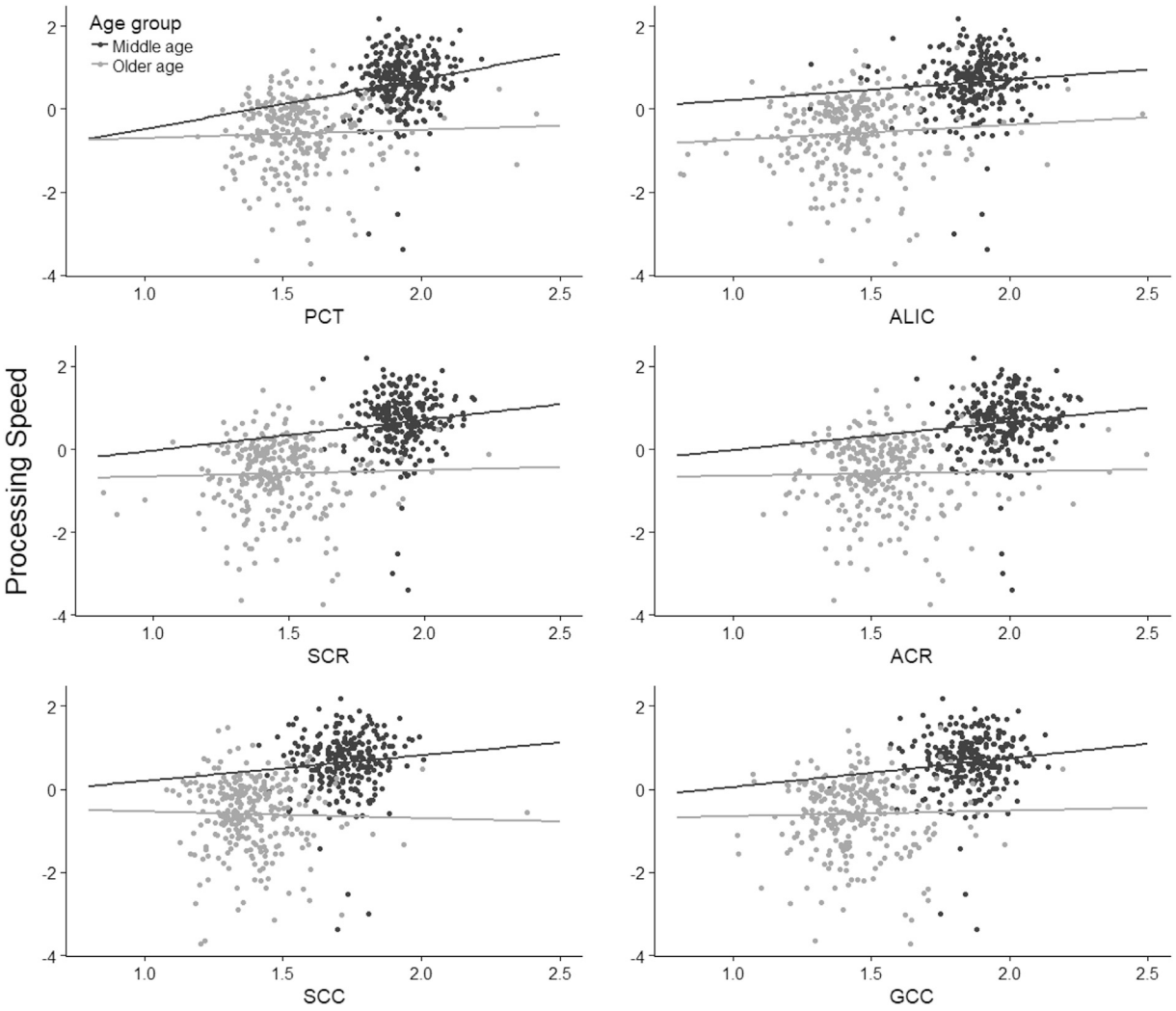


**Fig. 3.** Scatterplots of processing speed component as a function of estimated myelin content within each of the six selected tracts. ACR = anterior corona radiata; SCR = superior corona radiata; PCT = pontine crossing tract; ALIC = anterior limb of the internal capsule; GCC = genu of the corpus callosum; SCC = splenium of the corpus callosum.

the ALIC ($F = 44.438$, $p < .001$, $\eta_p^2 = 0.074$), GCC ($F = 24.931$, $p < .001$, $\eta_p^2 = 0.043$) and SCC ($p < .001$, $\eta_p^2 = 0.130$), whereas the reverse was found within the ACR ($F = 31.525$, $p < .001$, $\eta_p^2 = 0.053$), SCR ($F = 28.425$, $p < .001$, $\eta_p^2 = 0.048$) and PCT ($p < .001$, $\eta_p^2 = 0.317$). A significant hemisphere by AgeG interaction effect found within the GCC ($F = 58.146$, $p < .001$, $\eta_p^2 = 0.094$) revealed that while the right hemisphere had less MYE within the MA group, the left hemisphere had less MYE within the OA group. A significant hemisphere by sex interaction was also found within the GCC ($F = 10.626$, $p = .001$, $\eta_p^2 = 0.019$), with the left hemisphere having higher MYE within females, whereas no significant difference was found within males. All significant main effects and interactions for hemisphere survived Holm-Bonferroni correction for multiple comparisons.

### 3.9.2. Hemispheric asymmetries in MYE as a predictor of PS

The laterality index of the SCC ($\beta = 0.018$, $p = .002$) was a significant predictor of PS. As such, left and right SCC were examined in separate regression models (Table 3). Analyses revealed that the left SCC was a significant predictor of PS. One SD higher in the MYE of the left SCC was associated with 2.20% higher PS scores. This was a robust finding as the association remained significant after controlling for all covariates and survived Holm-Bonferroni correction for multiple comparisons. The right SCC was not a significant predictor in either models, and no significant interaction effects were detected.

**Table 3**
Hierarchical linear regression using MYE of the left and right SCC to predict PS.

| ROI | Model 1[a] | Model 2[a,b] | | | Model 3[a,b,c] | | |
|---|---|---|---|---|---|---|---|
| | $R^2$ | $\Delta R^2$ | β | *p* | $\Delta R^2$ | β | *p* |
| Left SCC | .416 | .010 | **.473** | **.003**** | .014 | **.504** | **.002**** |
| Right SCC | .416 | .001 | .124 | .464 | .013 | .130 | .442 |

** Significant at $p < .01$. Significant p-values and corresponding β values are given in bold.
[a] Model includes AgeG, AgeC, Sex and Education.
[b] Model includes MYE (mean T1w/T2w) of ROI.
[c] Model includes alcohol consumption, smoking, physical activity, hypertension, presence of APO*E4 genotype, depressive symptomology.

### 3.9.3. Total brain white matter MYE as a predictor of PS

As all examined tracts showed a trend towards higher MYE predicting faster PS, MYE of total brain white matter was examined as a predictor of PS. After controlling for AgeG, AgeC, Sex and Education, total brain white matter MYE was not a significant predictor of PS ($\Delta R^2 < 0.001$, $\beta = 0.149$, $p = .603$).

#### 3.9.4. White matter hyperintensities as a confounding factor

To ensure that white matter hyperintensities were not a confounding factor in our analyses, we computed the partial correlation between total white matter hypo-intensity volume (calculated using automated Freesurfer segmentation on T1-w images; Fischl et al., 2002) and total brain white matter MYE. After controlling for AgeG, there was no significant relationship between white matter hypo-intensity volume and total brain white matter MYE ($r = -0.048$, $p = .270$).

#### 3.9.5. Partial correlations between estimated myelin content and individual tests of PS

To determine which individual tests of PS were best predicted by the MYE of the ALIC and left SCC, post-hoc partial correlations between the two tracts and the five different tests of PS were computed, controlling for AgeG, AgeC, Sex and Education. To meet assumptions of normality and assess relative contributions, the z-scores for each test were used. Partial correlations revealed that, SDMT was the test most strongly correlated with the MYE of the ALIC ($r = 0.093$, $p = .037$), followed by CRT ($r = -0.073$, $p = .103$), SRT ($r = -0.050$, $p = .264$), TMT-A ($r = -0.054$, $p = .231$) and PP ($r = -0.008$, $p = .852$). Whereas for the left SCC, TMT-A was most strongly correlated ($r = -0.121$, $p = .007$), followed by CRT ($r = -0.108$, $p = .016$), SRT ($r = -0.089$, $p = .047$), PP ($r = 0.057$, $p = .203$) and SDMT ($r = 0.049$, $p = .273$).

## 4. Discussion

The present study investigated whether myelin content estimated *in vivo* (MYE) within major white matter tracts is predictive of PS in a sample of healthy community-dwelling adults and whether lower MYE could be detected in older compared to younger individuals. This study's main findings were that higher MYE in the ALIC and the left SCC significantly predicted faster PS scores and that MYE was lower in older than younger individuals.

### 4.1. Between-tract differences in mean T1w/T2w

Our findings within the corpus callosum showing that the genu has higher estimated myelin content than the splenium are consistent with previous research and histology studies (Aboitiz et al., 1992; Lee et al., 2014). However, while past studies have found the ALIC to have the highest myelin content within white matter areas (Whittall et al., 1997; Ganzetti et al., 2014), we found the ACR to have the highest MYE. As the sample used in the current study spans a substantially narrower and older age range than that of previous studies, it is possible this discrepancy represents aging-related myelin loss. Supporting this hypothesis, we found that the ALIC showed one of the largest estimated difference in MYE (24.06%) between the OA and MA group. In addition, the MA group had significantly higher T1w/T2w values in all six tracts, which is consistent with the previously reported trajectory of brain myelin content which begins to decline soon after mid-life (age 35–40; Bartzokis et al., 2003, 2010).

### 4.2. MYE predicts PS

While lower MYE has been demonstrated in clinical groups, and higher MYE within the cortex is correlated with performance stability on speeded tasks (Grydeland et al., 2013), to our knowledge this is the first study to utilise the T1-w/T2-w ratio to demonstrate an association between higher sub-cortical MYE and faster PS in generally healthy community-living individuals. These results support the claim that the higher speed of signal transmission provided by myelin can predict better outcomes within the cognitive domain of PS, even in healthy adults who are not likely to have marked myelin degradation similar to that found in clinical samples. Further, the results found were robust as they remained significant even after controlling for socio-demographic, health, genetic covariates and multiple comparisons.

The association between higher MYE and faster PS was found to be significant in the ALIC and left SCC and consistent trends were found in all tracts investigated. As opposed to previous research that used less specific measures of white mater integrity to show a global effect on processing speed (Penke et al., 2010; Kerchner et al., 2012), we found that total brain white matter MYE did not predict PS. Accordingly, these effects are likely to be specific and localised.

The ALIC is known for high myelin content, connecting the prefrontal cortex to thalamic nuclei, and the motor cortex to the anterior horn of the spinal cord (Mai et al., 2015). While the cognitive tests used within the current study primarily measure PS, they do not assess this property in relation to a single function and may reflect axonal conduction contributing to a variety of motor, perceptual and cognitive processes. As such, loss of myelin within the ALIC may result in the disruption of cognitive processes reliant on different circuits. Thus, since the cortico-thalamic circuit contributes to a range of cognitive processes that include learning and memory, inhibitory control, decision-making, and the control of visual orienting responses (Haber and Calzavara, 2009), differences in myelin content of its fibres may modulate performance of these processes. Alternatively, since the cortico-spinal circuit forms the major motor control pathway, the slowing of signals travelling through this circuit could result in the slowing of PS and psychomotor response seen in the current study. In support of this, myelin degradation and axonal damage within the ALIC has been linked with motor impairment in multiple sclerosis patients (Lee et al., 2000) and PS deficits in non-demented older adults (O'brien et al., 2002). Our finding within the ALIC is in agreement with previous research that has used diffusion imaging measures to show that the integrity of the ALIC is a significant predictors of PS (Salami et al., 2012).

Importantly, the speed at which an electrical signal travels along an axon is directly related to the degree and quality of myelin (Seidl, 2014). Temporal efficacy is essential within neural circuits to ensure computations are completed on time and synchronously. Evidence suggests that myelin from later-differentiating oligodendrocytes, such as those found in the ALIC, are less effective and more vulnerable to the age-related effects of inflammation and oxidative stress (Brickman et al., 2012; Kohama et al., 2012). If neural efficacy is compromised due to degradation of myelin sheath in vulnerable areas, like the ALIC, it may result in cognitive and behavioural slowing, such as that seen in the current study.

In addition to the ALIC, the MYE of the left SCC significantly predicted PS, while that of the GCC did not. This finding is not in agreement with previous research which has used less specific diffusion and transverse relaxometry imaging methods to show that frontal regions such as the GCC are more strongly associated with PS than posterior regions such as the SCC (Lu et al., 2011, 2013; Salami et al., 2012). The SCC is a major commissural tract, accommodating interhemispheric connections between visual, parietal and posterior cingulate areas (Knyazeva, 2013), and has previously been associated with PS, in that age-related volume loss (Anstey et al., 2007) and white-matter hyper-intensities within the SCC have been found to be associated with slower speed of processing (Park et al., 2014). These age-related findings may be due to increased interhemispheric synchronisation facilitated by the heavily myelinated fibres of the SCC (Hinkley et al., 2012). As such, the current study suggests that age-related PS disruptions associated with the SCC may be due to myelin degradation within this structure. However, only the MYE of the left SCC was a significant predictor of PS. While it is possible that this lateralised finding is due to noise or measurement error, the left hemisphere, and in particular the left SCC has typically been found to be more prone to neurodegeneration (Yoon et al., 2011). Additionally, in Alzheimer's disease, cortical atrophy begins earlier and progresses faster within the left hemisphere (Thompson et al., 2007; Minkova et al., 2017). Consequently, the laterality effect observed in the present study may reflect a greater vulnerability of the left SCC to the adverse effects of ageing.

It is of clinical utility to determine which of the five individual tests of PS would be best predicted by MYE deficits with in the ALIC and left SCC.

Post-hoc analysis showed that the SDMT and TMT-A were most strongly correlated with the MYE of the ALIC and left SCC respectively. One of the major aspects that differentiates these two tests from the others is increased cognitive complexity – as opposed to SRT, CRT, and PP which are primarily reliant on precise motor skills and visual feedback. This is consistent with the fact that the ALIC contributes to the fronto-thalamic circuitry which is involved in complex cognition such as executive functions.

### 4.3. Strengths and limitations

One of the primary strengths of this study was the robust measurement of PS. By extracting a latent measure of PS from five different individual tests, unwanted variance relating to other properties was minimised by analysing common aspects of tasks that vary in methodology but load heavily on PS (Cepeda et al., 2013). In addition, the large sample size and carefully selected covariates were also substantial strengths.

Despite this, the narrow age-range of the two groups and the relative good health of our sample may have restricted variance in myelin content that might be otherwise expected in a population with a greater age range or in a clinical sample. Additionally, due to the cross-sectional design used, causal inferences on the association between the T1w/T2w signal and PS cannot be drawn. Future studies should therefore apply this technique to longitudinal datasets to determine both lifelong myelin content trajectories and test their associations across a greater range of cognitive domains such as memory and attention, which may also be materially affected by progressive age-related myelin loss.

It should be noted, that due to the complexity of neural circuits, lower myelin content in specific white matter tracts may not necessarily be associated with slower PS. However, the white matter tracts used within the current study were selected as they facilitate information transfer between brain regions known to be implicated in functions sensitive to PS. Therefore, it would be expected that variability in myelin content in these regions would impact PS.

In addition, while the measure of myelin content used in this study has shown correlation to myelin levels of post-mortem brains using immunocytochemistry (Nakamura et al., 2017), our understanding of it will benefit from further validation against histological measures which allow us to understand the relative contribution of other factors such as iron levels and inflammation. However, a recent study demonstrated that within a small sample, the measure had high test-retest reliability (Arshad et al., 2017). Future studies should continue to aim to directly validate the origin of the T1w/T2w signal by using histology techniques in post-mortem animal and human models.

## 5. Conclusion

Estimating brain myelin content using the T1w/T2w technique is relatively easy to implement and does not require lengthy acquisition times or a complex processing pipeline; therefore, it is a practical method to identify age-related brain changes and should be further investigated in future research as a biomarker for neurocognitive diseases. Using this technique, the current study is the first to demonstrate *in vivo* that higher MYE of white matter tracts assessed with a specific and sensitive measure is associated with faster PS in healthy adults, even after controlling for socio-demographic, health and genetic variables.

## Acknowledgements

The authors declare no competing financial interests. The authors are grateful to Anthony Jorm, Helen Christensen, Peter Butterworth, Andrew McKinnon, and the PATH project interviewers. The study was supported by NHMRC Grant 973302, 179805, 157125, 1063907. Nicolas Cherbuin is funded by ARC Future Fellowship no. 120100227 and Kaarin Anstey by NHMRC Fellowship 1002560. This research was supported by the Australian Research Council Centre of Excellence in Population Ageing Research (project no. CE110001029). This research was partly undertaken on the National Computational Infrastructure (NCI) facility in Canberra, Australia, which is supported by the Australian Commonwealth Government.

## References

Aboitiz, F., Scheibel, A.B., Fisher, R.S., Zaidel, E., 1992. Fiber composition of the human corpus callosum. Brain Res. 598, 143–153.
Anstey, K.J., Low, L.-F., Christensen, H., Sachdev, P., 2009. Level of cognitive performance as a correlate and predictor of health behaviors that protect against cognitive decline in late life: the path through life study. Intelligence 37, 600–606.
Anstey, K.J., Mack, H.A., Christensen, H., Li, S.-C., Reglade-Meslin, C., Maller, J., Kumar, R., Dear, K., Easteal, S., Sachdev, P., 2007. Corpus callosum size, reaction time speed and variability in mild cognitive disorders and in a normative sample. Neuropsychologia 45, 1911–1920.
Anstey, K.J., Christensen, H., Butterworth, P., Easteal, S., Mackinnon, A., Jacomb, T., Maxwell, K., Rodgers, B., Windsor, T., Cherbuin, N., 2012. Cohort profile: the PATH through life project. Int. J. Epidemiol. 41, 951–960.
Arshad, M., Stanley, J.A., Raz, N., 2017. Test–retest reliability and concurrent validity of in vivo myelin content indices: myelin water fraction and calibrated T1w/T2w image ratio. Hum. Brain Mapp. 38, 1780–1790.
Babor, T.F., Higgins-Biddle, J.C., Saunders, J.B., Monteiro, M.G., 2001. The alcohol use disorders identification test. Guidelines for use in primary care 2.
Bartzokis, G., 2004. Age-related myelin breakdown: a developmental model of cognitive decline and Alzheimer's disease. Neurobiol. Aging 25, 5–18.
Bartzokis, G., Cummings, J.L., Sultzer, D., Henderson, V.W., Nuechterlein, K.H., Mintz, J., 2003. White matter structural integrity in healthy aging adults and patients with Alzheimer disease: a magnetic resonance imaging study. Arch. Neurol. 60, 393–398.
Bartzokis, G., Lu, P.H., Geschwind, D.H., Tingus, K., Huang, D., Mendez, M.F., Edwards, N., Mintz, J., 2007. Apolipoprotein E affects both myelin breakdown and cognition: implications for age-related trajectories of decline into dementia. Biol. Psychiatr. 62, 1380–1387.
Bartzokis, G., Lu, P.H., Tingus, K., Mendez, M.F., Richard, A., Peters, D.G., Oluwadara, B., Barrall, K.A., Finn, J.P., Villablanca, P., 2010. Lifespan trajectory of myelin integrity and maximum motor speed. Neurobiol. Aging 31, 1554–1562.
Bartzokis, G., Lu, P.H., Heydari, P., Couvrette, A., Lee, G.J., Kalashyan, G., Freeman, F., Grinstead, J.W., Villablanca, P., Finn, J.P., 2012. Multimodal magnetic resonance imaging assessment of white matter aging trajectories over the lifespan of healthy individuals. Biol. Psychiatr. 72, 1026–1034.
Beer, A., Biberacher, V., Schmidt, P., Righart, R., Buck, D., Berthele, A., Kirschke, J., Zimmer, C., Hemmer, B., Mühlau, M., 2016. Tissue damage within normal appearing white matter in early multiple sclerosis: assessment by the ratio of T1-and T2-weighted MR image intensity. J. Neurol. 263, 1495–1502.
Brickman, A.M., Meier, I.B., Korgaonkar, M.S., Provenzano, F.A., Grieve, S.M., Siedlecki, K.L., Wasserman, B.T., Williams, L.M., Zimmerman, M.E., 2012. Testing the white matter retrogenesis hypothesis of cognitive aging. Neurobiol. Aging 33, 1699–1715.
Bunce, D., Macready, A., 2005. Processing speed, executive function, and age differences in remembering and knowing. The Quarterly Journal of Experimental Psychology Section A 58, 155–168.
Cepeda, N.J., Blackwell, K.A., Munakata, Y., 2013. Speed isn't everything: complex processing speed measures mask individual differences and developmental changes in executive control. Dev. Sci. 16, 269–286.
Cerella, J., Hale, S., 1994. The rise and fall in information-processing rates over the life span. Acta Psychol. 86, 109–197.
Cherbuin, N., Sachdev, P., Anstey, K.J., 2010. Neuropsychological predictors of transition from healthy cognitive aging to mild cognitive impairment: the PATH through life study. Am. J. Geriatr. Psychiatr. 18, 723–733.
Christensen, H., Batterham, P.J., Mackinnon, A.J., Jorm, A.F., Mack, H.A., Mather, K.A., Anstey, K.J., Sachdev, P.S., Easteal, S., 2008. The association of APOE genotype and cognitive decline in interaction with risk factors in a 65–69 year old community sample. BMC Geriatr. 8, 14.
Davis, S.W., Dennis, N.A., Buchler, N.G., White, L.E., Madden, D.J., Cabeza, R., 2009. Assessing the effects of age on long white matter tracts using diffusion tensor tractography. Neuroimage 46, 530–541.
de Schotten, M.T., Bizzi, A., Dell'Acqua, F., Allin, M., Walshe, M., Murray, R., Williams, S.C., Murphy, D.G., Catani, M., 2011. Atlasing location, asymmetry and inter-subject variability of white matter tracts in the human brain with MR diffusion tractography. Neuroimage 54, 49–59.
Demaree, H.A., DeLuca, J., Gaudino, E.A., Diamond, B.J., 1999. Speed of information processing as a key deficit in multiple sclerosis: implications for rehabilitation. J Neurology Neurosurgery & Psychiatry 67, 661–663.
Finkel, D., Reynolds, C.A., McArdle, J.J., Pedersen, N.L., 2007. Age changes in processing speed as a leading indicator of cognitive aging. Psychol. Aging 22, 558.
Fischl, B., Salat, D.H., Busa, E., Albert, M., Dieterich, M., Haselgrove, C., Van Der Kouwe, A., Killiany, R., Kennedy, D., Klaveness, S., 2002. Whole brain segmentation: automated labeling of neuroanatomical structures in the human brain. Neuron 33, 341–355.
Ganzetti, M., Wenderoth, N., Mantini, D., 2014. Whole brain myelin mapping using T1- and T2-weighted MR imaging data. Front. Hum. Neurosci. 8, 671.

Ganzetti, M., Wenderoth, N., Mantini, D., 2015. Mapping pathological changes in brain structure by combining T1-and T2-weighted MR imaging data. Neuroradiology 57, 917–928.
Glasser, M.F., Van Essen, D.C., 2011. Mapping human cortical areas in vivo based on myelin content as revealed by T1-and T2-weighted MRI. J. Neurosci. 31, 11597–11616.
Glasser, M.F., Goyal, M.S., Preuss, T.M., Raichle, M.E., Van Essen, D.C., 2014. Trends and properties of human cerebral cortex: correlations with cortical myelin content. Neuroimage 93, 165–175.
Goldberg, D., Bridges, K., Duncan-Jones, P., Grayson, D., 1988. Detecting anxiety and depression in general medical settings. Bmj 297, 897–899.
Grydeland, H., Walhovd, K.B., Tamnes, C.K., Westlye, L.T., Fjell, A.M., 2013. Intracortical myelin links with performance variability across the human lifespan: results from T1- and T2-weighted MRI myelin mapping and diffusion tensor imaging. J. Neurosci. 33, 18618–18630.
Haber, S.N., Calzavara, R., 2009. The cortico-basal ganglia integrative network: the role of the thalamus. Brain Res. Bull. 78, 69–74.
Hinkley, L.B., Marco, E.J., Findlay, A.M., Honma, S., Jeremy, R.J., Strominger, Z., Bukshpun, P., Wakahiro, M., Brown, W.S., Paul, L.K., 2012. The role of corpus callosum development in functional connectivity and cognitive processing. PLos One 7, e39804.
Holm, S., 1979. A simple sequentially rejective multiple test procedure. Scand. J. Stat. 65–70.
Ishida, T., Donishi, T., Iwatani, J., Yamada, S., Takahashi, S., Ukai, S., Shinosaki, K., Terada, M., Kaneoke, Y., 2017. Elucidating the aberrant brain regions in bipolar disorder using T1-weighted/T2-weighted magnetic resonance ratio images. Psychiatr. Res. Neuroimaging 263, 76–84.
Iwatani, J., Ishida, T., Donishi, T., Ukai, S., Shinosaki, K., Terada, M., Kaneoke, Y., 2015. Use of T1-weighted/T2-weighted magnetic resonance ratio images to elucidate changes in the schizophrenic brain. Brain and behavior 5.
Kerchner, G.A., Racine, C.A., Hale, S., Wilheim, R., Laluz, V., Miller, B.L., Kramer, J.H., 2012. Cognitive processing speed in older adults: relationship with white matter integrity. PLos One 7, e50425.
Knyazeva, M.G., 2013. Splenium of corpus callosum: patterns of interhemispheric interaction in children and adults. Neural Plasticity 2013, 63943.
Kohama, S.G., Rosene, D.L., Sherman, L.S., 2012. Age-related changes in human and non-human primate white matter: from myelination disturbances to cognitive decline. Age 34, 1093–1110.
Lamont, A.J., Mortby, M.E., Anstey, K.J., Sachdev, P.S., Cherbuin, N., 2014. Using sulcal and gyral measures of brain structure to investigate benefits of an active lifestyle. Neuroimage 91, 353–359.
Lee, B., Zhu, X., Li, X., Chen, W., 2014. Quantitative assessment of microstructure properties of human corpus callosum using parametric T1 and myelin imaging. In: Proceedings of the International Society for Magnetic Resonance in Medicine, p. 3236.
Lee, M.A., Blamire, A.M., Pendlebury, S., Ho, K.-H., Mills, K.R., Styles, P., Palace, J., Matthews, P.M., 2000. Axonal injury or loss in the internal capsule and motor impairment in multiple sclerosis. Arch. Neurol. 57, 65–70.
Lee, T., Crawford, J.D., Henry, J.D., Trollor, J.N., Kochan, N.A., Wright, M.J., Ames, D., Brodaty, H., Sachdev, P.S., 2012. Mediating effects of processing speed and executive functions in age-related differences in episodic memory performance: a cross-validation study. Neuropsychology 26, 776.
Leppert, I.R., Almli, C.R., McKinstry, R.C., Mulkern, R.V., Pierpaoli, C., Rivkin, M.J., Pike, G.B., 2009. T2 relaxometry of normal pediatric brain development. J. Magn. Reson. Imag. 29, 258–267.
Lu, P.H., Lee, G.J., Tishler, T.A., Meghpara, M., Thompson, P.M., Bartzokis, G., 2013. Myelin breakdown mediates age-related slowing in cognitive processing speed in healthy elderly men. Brain Cognit. 81, 131–138.
Lu, P.H., Lee, G.J., Raven, E.P., Tingus, K., Khoo, T., Thompson, P.M., Bartzokis, G., 2011. Age-related slowing in cognitive processing speed is associated with myelin integrity in a very healthy elderly sample. J. Clin. Exp. Neuropsychol. 33, 1059–1068.
Madden, D.J., Whiting, W.L., Huettel, S.A., White, L.E., MacFall, J.R., Provenzale, J.M., 2004. Diffusion tensor imaging of adult age differences in cerebral white matter: relation to response time. Neuroimage 21, 1174–1181.
Mai, J.K., Majtanik, M., Paxinos, G., 2015. Atlas of the Human Brain. Academic Press.
Minkova, L., Habich, A., Peter, J., Kaller, C.P., Eickhoff, S.B., Klöppel, S., 2017. Gray matter asymmetries in aging and neurodegeneration: a review and meta-analysis. Hum. Brain Mapp. 38, 5890–5904.
Nakamura, K., Chen, J.T., Ontaneda, D., Fox, R.J., Trapp, B.D., 2017. T1-/T2-weighted ratio differs in demyelinated cortex of multiple sclerosis. Annals of Neurology.
Nieuwenhuys, R., Broere, C.A., 2017. A map of the human neocortex showing the estimated overall myelin content of the individual architectonic areas based on the studies of Adolf Hopf. Brain Struct. Funct. 222, 465–480.
O'brien, J.T., Wiseman, R., Burton, E.J., Barber, B., Wesnes, K., Saxby, B., Ford, G.A., 2002. Cognitive associations of subcortical white matter lesions in older people. Ann. N. Y. Acad. Sci. 977, 436–444.
Ocklenburg, S., Friedrich, P., Güntürkün, O., Genç, E., 2016. Intrahemispheric white matter asymmetries: the missing link between brain structure and functional lateralization? Rev. Neurosci. 27, 465–480.
Oishi, K., Faria, A., Jiang, H., Li, X., Akhter, K., Zhang, J., Hsu, J.T., Miller, M.I., van Zijl, P.C., Albert, M., 2009. Atlas-based whole brain white matter analysis using large deformation diffeomorphic metric mapping: application to normal elderly and Alzheimer's disease participants. Neuroimage 46, 486–499.
Park, M.-K., Hwang, S.-H., Jung, S., Hong, S.-S., Kwon, S.-B., 2014. Lesions in the splenium of the corpus callosum: clinical and radiological implications. Neurol. Asia 19.
Penke, L., Maniega, S.M., Murray, C., Gow, A.J., Hernández, M.C.V., Clayden, J.D., Starr, J.M., Wardlaw, J.M., Bastin, M.E., Deary, I.J., 2010. A general factor of brain white matter integrity predicts information processing speed in healthy older people. J. Neurosci. 30, 7569–7574.
Racine, A.M., Adluru, N., Alexander, A.L., Christian, B.T., Okonkwo, O.C., Oh, J., Cleary, C.A., Birdsill, A., Hillmer, A.T., Murali, D., 2014. Associations between white matter microstructure and amyloid burden in preclinical Alzheimer's disease: a multimodal imaging investigation. NeuroImage: Clinical 4, 604–614.
Ramagopalan, S.V., Dobson, R., Meier, U.C., Giovannoni, G., 2010. Multiple sclerosis: risk factors, prodromes, and potential causal pathways. Lancet Neurol. 9, 727–739.
Reitan, R.M., 1958. Validity of the Trail Making Test as an indicator of organic brain damage. Percept. Mot. Skills 8, 271–276.
Salami, A., Eriksson, J., Nilsson, L.-G., Nyberg, L., 2012. Age-related white matter microstructural differences partly mediate age-related decline in processing speed but not cognition. Biochim. Biophys. Acta (BBA) - Mol. Basis Dis. 1822, 408–415.
Salthouse, T.A., Fristoe, N., Rhee, S.H., 1996. How localized are age-related effects on neuropsychological measures? Neuropsychology 10, 272.
Seidl, A.H., 2014. Regulation of conduction time along axons. Neuroscience 276, 126–134.
Strauss, E., Sherman, E.M., Spreen, O., 2006. A Compendium of Neuropsychological Tests: Administration, Norms, and Commentary. American Chemical Society.
Takao, H., Hayashi, N., Ohtomo, K., 2011. White matter asymmetry in healthy individuals: a diffusion tensor imaging study using tract-based spatial statistics. Neuroscience 193, 291–299.
Thompson, P.M., Hayashi, K.M., Dutton, R.A., CHIANG, M.C., Leow, A.D., Sowell, E.R., De Zubicaray, G., Becker, J.T., Lopez, O.L., Aizenstein, H.J., 2007. Tracking Alzheimer's disease. Ann. N. Y. Acad. Sci. 1097, 183–214.
Tiffin, J., Asher, E.J., 1948. The Purdue Pegboard: norms and studies of reliability and validity. J. Appl. Psychol. 32, 234.
Toga, A.W., Thompson, P.M., 2003. Mapping brain asymmetry. Nat. Rev. Neurosci. 4, 37.
Turken, U., Whitfield-Gabrieli, S., Bammer, R., Baldo, J.V., Dronkers, N.F., Gabrieli, J.D., 2008. Cognitive processing speed and the structure of white matter pathways: convergent evidence from normal variation and lesion studies. Neuroimage 42, 1032–1044.
Welker, K.M., Patton, A., 2012. Assessment of normal myelination with magnetic resonance imaging. In: Seminars in Neurology. Thieme Medical Publishers, pp. 015–028.
Whittall, K.P., Mackay, A.L., Graeb, D.A., Nugent, R.A., Li, D.K., Paty, D.W., 1997. In vivo measurement of T2 distributions and water contents in normal human brain. Magn. Reson. Med. 37, 34–43.
Winston, G.P., 2012. The physical and biological basis of quantitative parameters derived from diffusion MRI. Quant. Imag. Med. Surg. 2, 254–265.
Yoon, B., Shim, Y.-S., Hong, Y.-J., Koo, B.-B., Kim, Y.-D., Lee, K.-O., Yang, D.-W., 2011. Comparison of diffusion tensor imaging and voxel-based morphometry to detect white matter damage in Alzheimer's disease. J. Neurol. Sci. 302, 89–95.